Biogeosciences Discuss., 12, 9243–9273, 2015
www.biogeosciences-discuss.net/12/9243/2015/
doi:10.5194/bgd-12-9243-2015

Biogeosciences Discussions
Open Access

Influence of mesoscale eddies on the distribution of nitrous oxide in the eastern tropical South Pacific

D. L. Arévalo-Martínez[1], A. Kock[1], C. R. Löscher[2], R. A. Schmitz[2], L. Stramma[1], and H. W. Bange[1]

[1]GEOMAR Helmholtz Centre for Ocean Research Kiel, Düsternbrooker Weg 20, 24105 Kiel, Germany
[2]Institute of Microbiology, Christian Albrechts University of Kiel, Am Botanischen Garten 1–9, 24118 Kiel, Germany

Received: 05 May 2015 – Accepted: 03 June 2015 – Published: 19 June 2015

Correspondence to: D. L. Arévalo-Martínez (darevalo@geomar.de)

Published by Copernicus Publications on behalf of the European Geosciences Union.

Abstract

Recent observations in the eastern tropical South Pacific (ETSP) demonstrated the key role of meso- and submesoscale processes (e.g. eddies) in shaping its hydrographic and biogeochemical properties. Off Peru, elevated primary production from coastal upwelling in combination with sluggish ventilation of subsurface waters fuels a prominent oxygen minimum zone (OMZ). Given that nitrous oxide (N_2O) production/consumption processes on the water column are sensitive to oxygen (O_2) concentrations, the ETSP is a region of particular interest to investigate its source-sink dynamics. To date, no detailed surveys linking mesoscale processes and N_2O distributions as well as their relevance to nitrogen (N) cycling are available. In this study, we present the first measurements of N_2O across three mesoscale eddies (two mode water or anticyclonic and one cyclonic) which were identified, tracked and sampled during two surveys carried out in the ETSP in November-December 2012. A "two peak" structure was observed for N_2O, wherein the two maxima coincide with the upper and lower boundaries of the OMZ, indicating active nitrification and partial denitrification. This was further supported by the abundances of the key gene for nitrification *amoA* and the gene marker for N_2O production during denitrification, *nirS*. Conversely, we found strong N_2O depletion in the core of the OMZ ($O_2 < 5\,\mu mol\,L^{-1}$) to be consistent with nitrite (NO_2^-) accumulation and low levels of nitrate (NO_3^-), thus suggesting active denitrification. N_2O depletion within the OMZ's core was substantially higher in the center of mode water eddies, supporting the view that eddy activity enhances N-loss processes off Peru, in particular near the shelf break where nutrient-rich, productive waters from upwelling are trapped before being transported offshore. Analysis of eddies during their propagation towards the open ocean showed that, in general, "aging" of mesoscale eddies tends to decrease N_2O concentrations through the water column in response to reduced supply of material to fuel N-loss, although hydrographic variability might also significantly impact the pace of the production/consumption pathways for N_2O. Our results demonstrate the relevance of mode water eddies for N_2O distribution, thereby improving our

BGD
12, 9243–9273, 2015

understanding of the N-cycling processes, which are of crucial importance in times of climate change and ocean deoxygenation.

1 Introduction

Nitrous oxide (N_2O) is an atmospheric trace gas which strongly affects Earth's climate both by contributing to the greenhouse effect and by its role as a major ozone-depleting substance (Ravishankara et al., 2009; Myhre et al., 2013). The ocean is a net source of N_2O to the atmosphere accounting for about one third of the total natural source (Myhre et al., 2013), and therefore, the investigation of its formation pathways under changing oceanic regimes is relevant for any future predictions of how the nitrogen (N) cycle will react to future climate change. N_2O is mainly produced by microbial nitrification and denitrification, with particularly high yields under low oxygen (O_2) conditions (Goreau et al., 1980; Naqvi et al., 2010; Löscher et al., 2012; Bakker et al., 2014) such as those found in oxygen minimum zones (OMZ) of the tropical oceans. In the eastern tropical South Pacific (ETSP) a prominent OMZ is formed and maintained by the close coupling between elevated primary production fueled by coastal upwelling and weak ventilation of intermediate waters (Karstensen et al., 2008). Although elevated N_2O production in these subsurface low-O_2 waters could supply as much as 25–50 % of the global ocean source (Suntharalingam et al., 2000), it has been shown that when O_2 concentrations fall below about 5 µmol L^{-1} (in the OMZ's core) N_2O consumption through denitrification ($NO_3^- \rightarrow NO_2^- \rightarrow NO \rightarrow N_2O \rightarrow N_2$) takes place, and therefore these waters may act as a net sink for this gas (Codispoti and Christensen, 1985; Löscher et al., 2015). Hence, OMZ's have a significant role in the marine N cycle not only due to their influence on the subsurface production of climate relevant trace gases such as N_2O (Paulmier et al., 2008; Codispoti, 2010; Capone and Hutchins, 2013) but also because of their contribution to the loss of bioavailable fixed N (Kalvelage et al., 2013; Dalsgaard et al., 2014). Further ocean deoxygenation as well as expansion of the OMZs worldwide could in turn increase the volume of waters in which N-loss takes place (Stramma et

BGD
12, 9243–9273, 2015

al., 2010; Deutsch et al., 2011), thereby intensifying N limitation of primary production and reducing ocean's ability to sequester atmospheric CO_2 (Falkowski, 1997).

Recent observations have demonstrated the key role of meso- and submesoscale processes in shaping hydrographic and biogeochemical properties of the ETSP (Stramma et al., 2013, 2014). Along the Peruvian coast, instabilities of the main current flow lead to the formation of nonlinear mesoscale eddies which propagate offshore from the site of formation, significantly contributing to the cross-shelf transport of heat, mass, momentum and biogeochemical properties (Chelton et al., 2007; Chaigneau et al., 2008). Likewise, offshore propagation of mesoscale eddies has been shown to increase the spatial extent of the high productivity area of the coastal upwelling (Correa-Ramirez et al., 2007; Chelton et al., 2011), implying their relevance in the export of carbon to the open ocean. Provided that downward transport of organic matter is an essential control of the marine N cycle (Kalvelage et al., 2013), it is of interest to investigate potential changes in N_2O distribution within mesoscale eddies. Although such mesoscale features in the OMZ off Peru have been identified as locations of enhanced N-loss (Altabet et al., 2012; Stramma et al., 2013), to date no detailed surveys linking mesoscale eddies and N_2O as well as their relevance to N-cycling are available.

The main goal of this study is to present the first set of N_2O measurements collected across three mesoscale eddies which were tracked during the R/V *Meteor* cruises M90 and M91 in November-December 2012. Furthermore, we use a combination of N_2O concentrations and abundance of selected molecular markers (key genes) for its main formation pathways to elucidate the causes of the observed distribution. Finally, we compare the N_2O concentrations within the center of "young" and "old" mesoscale eddies in order to identify the net effect of their "aging" (offshore propagation).

2 Eddy surveys

The field work was conducted in November–December 2012 during the R/V *Meteor* cruises M90 and M91, which covered the open ocean and shelf areas off Peru (5–

BGD
12, 9243–9273, 2015

25° S, 75–86° W). Detailed physical and biogeochemical surveys of mesoscale eddies were carried out between 14–18° S and 75–84° W on 16 to 25 November and on 19 to 23 December. Based on near-real time satellite data of sea level height anomalies (SSHA) from Aviso (http://aviso.altimetry.fr/), it was possible to identify two mode water (anticyclonic) eddies at the shelf break (eddy A) and the open ocean (eddy B), as well as one cyclonic eddy (eddy C) in the open ocean. Likewise, SSHA data was used to track and revisit eddy A in order to investigate its property's distribution after it started to move westward across the shelf break (Fig. 1).

2.1 Oceanographic and biogeochemical measurements

Ocean velocities were recorded by means of two RDI OceanSurveyor acoustic Doppler current profilers (ADCP), which provided velocity data down to about 700 and 1200 m depth (75 and 38 kHz, respectively). Discrete water sampling as well as profiling of hydrographic properties was carried out by means of a Sea-Bird CTD/Rosette equipped with 10 L Niskin bottles and double sensors for temperature, conductivity and O_2. Seawater samples for discrete O_2 measurements were collected by drawing bubble-free samples from the CTD/Rosette system. O_2 concentrations of these samples were determined by the Winkler method (Hansen, 1999), and were used to calibrate the O_2 sensors. The overall precision of the O_2 discrete measurements was $\pm 0.45\,\mu mol\,L^{-1}$. Nitrate ($NO_3^-$), nitrite ($NO_2^-$) and phosphate ($PO_4^{-3}$) concentrations were measured on board by means of a QuAAtro auto-analyzer (SEAL Analytical GmbH, Germany) with an overall precision of $\pm 0.1\,\mu mol\,L^{-1}$ (NO_3^- and NO_2^-) and $\pm 0.02\,\mu mol\,L^{-1}$ (PO_4^{3-}). The N deficit (or N^*) was computed as: $[NO_3^-] + [NO_2^-] - 16 \times [PO_4^{-3}]$. Chlorophyll *a* (Chl *a*) concentrations were determined by the acetone extraction method followed by fluorometric analysis with a Trilogy® laboratory fluorometer (Welschmeyer, 1994). Turbidity was measured by means of a factory-calibrated Wetlabs Fluorometer/Turbidity sensor with sensitivity up to 0.01 NTU (Nephelometric Turbidity Units). Discrete N_2O samples were collected in 22 stations with emphasis on the upper 1000 m of the water col-

BGD
12, 9243–9273, 2015

umn. For this purpose, bubble-free, triplicate samples were collected in 20 mL brown glass flasks and sealed with rubber butyl septa and metallic caps to avoid any gas exchange. Subsequently, a headspace was created on each flask by injecting 10 mL helium (99.999 %, AirLiquide GmbH, Düsseldorf, Germany). Microbial activity within the samples was prevented by adding 50 µl of a 1:3 dilution of a saturated mercuric chloride ($HgCl_2$) solution. After an equilibration period of minimum two hours the samples were analyzed using a GC-ECD system (Hewlett Packard (HP) 5890 Series II gas chromatograph). The separation procedure was carried out in a stainless steel column (long: 1.83 m, external diameter: 3.2 mm, internal diameter: 2.2 mm) with a molecular sieve of 5 Å (W.R. Grace & Co. Conn., Columbia, USA). The GC-ECD was calibrated daily by using dilutions of at least three standard gas mixtures up to 10400 ppb (Deuste Steininger GmbH, Mühlheim, Germany). Standard gases with $N_2O < 1000$ ppb were calibrated in the department of atmospheric chemistry of the Max-Plank Institute for Biogeochemistry (Jena, Germany) against the NOAA 2006 scale, whereas for $N_2O > 1000$ ppb the gas molar fraction was determined by means of high-resolution measurements of a calibrated OA-ICOS analyzer (precision better than 0.3 ppb, Arévalo-Martínez, et al., 2013). Calculation of the N_2O concentrations was done as described by Walter et al. (2006). Our designation of particular stations to eddy cores and edges was based on the SSHA data and follows the criteria defined by Stramma et al. (2013).

2.2 Molecular genetic methods

Nucleic acids samples were collected by filtering up to 1 L of seawater (exact volumes were recorded and the filtration time was lower than 20 min) onto polycarbonate membrane filters with a pore size of 0.2 µm (Millipore). Immediately after collection, samples were frozen at −80 °C until further processing. Nucleic acids were extracted using DNA/RNA AllPrep Kit (Qiagen, Hildesheim, Germany) with additional 15 min cell lysis (10 mg mL^{-1} lysozyme in 10 mM Tris-EDTA, pH 8), and shock freezing in liquid nitrogen before extraction. Quantitative (*q*)PCR followed protocols in Löscher et al. (2014) ex-

BGD
12, 9243–9273, 2015

cept that a ViiA7 qPCR system (Life Technologies, Carlsbad, CA, USA) was used. The sensitivity level for the detection of ammonium monooxygenase (*amoA*) and hydrazine oxidoreductase (*hzo*) genes with this method is 4 copies L^{-1}, whereas for the nitrite reductase (*nirS*) gene is 1 copy L^{-1}.

3 Hydrographic and biogeochemical setting

The properties of the eddies investigated during the M90 (November 2012) and M91 (December 2012) cruises were described in detail by Stramma et al. (2013) and therefore only the main features are briefly mentioned here. The eddy A was centered at about 16° S, 76° W with the highest intensity (zonal and meridional velocities) in the upper 600 m. As a typical mode water eddy, lifting/deepening of the seasonal/main pycnocline could be observed (McGillicuddy et al., 2007), whereby O_2 was lower, and temperature and salinity were higher in the center of the eddy than at its edges (Fig. 2). Shoaling of the mixed layer depth in the center of the eddy A coincided with a high Chl *a* maximum at about 50 m depth and a up to 30 % reduction in O_2 concentrations. The outer western side of cross-shelf sections across eddy A also revealed the influence of coastal upwelling near the shelf break in the upper 180 m. However this feature was detached from the eddy itself as it is shown by temperature, O_2 and velocity distributions (Fig. 2). Meridional velocity distributions as well as temperature, salinity and density fields suggest that eddy A enclosed waters from the Peru-Chile Undercurrent (PCU) at the time of formation near the shelf (Stramma et al., 2013). The eddy B was centered in the open ocean at about 17° S, 83°30′ W. Although the velocity distribution was similar to that of eddy A (strong in the upper 600 m), rotational speeds were lower and the temperature, salinity and density anomalies (difference between stations at the center of the eddy and at its edges) were weaker than in eddy A. Moreover, in comparison with eddy A, the depth of uplifting isopycnals and the mixed layer depth were deeper in eddy B (Fig. 2). As a consequence, the Chl *a* maximum as well as the temperature and O_2 anomalies could be found 100 m deeper in eddy B than in eddy A. A trajectory

BGD
12, 9243–9273, 2015

analysis indicated that eddy B was formed near the shelf about five months before the time of sampling (i.e. 3 months older than eddy A); however a precise location could not be determined with our methods (Stramma et al., 2013). Eddy C was centered in the open ocean at 16°15′ S, 80°15′ W with maximum velocities at ca. 50 m depth, and a positive density anomaly over the upper 600 m. In contrast to the anticyclonic eddies A and B, temperature and salinity of eddy C were lower and density was higher in the center than in its edges (Fig. 2), although the magnitude of the anomalies was similar to those of eddy A (Stramma et al., 2013). Furthermore, O_2 concentrations were higher in the center of the eddy than in the edges and the size of the O_2 anomaly in the OMZ was larger than for eddy A, indicating ventilation of the OMZ with waters from below the main thermocline. Eddy C was formed at the coast but unlike the anticyclones it moved westward without staying at the shelf (Stramma et al., 2013).

4 Results and discussion

4.1 Depth distribution of N_2O

N_2O concentrations in the water column featured a two-peak structure with maxima N_2O concentrations at the upper and lower boundaries of the OMZ, and depletion at the OMZ's core (Fig. 3). Such pattern has been previously reported for the ETSP (Farías et al., 2007) and similar systems with prominent OMZs (Bange et al., 2001; Bange et al., 2010), and it is generally ascribed to alternating activity of microbial N_2O production/consumption pathways along the vertical O_2 gradients (Codispoti and Christensen, 1985). Although elevated N_2O concentrations were observed in near-surface waters (up to 88 nmol L^{-1}) of the northwestern edge of eddy A, at the time of sampling the eddy was already detached from the coast and thus these high concentrations could be rather associated to coastal upwelling. In agreement with the distribution of physical properties (Fig. 2), the vertical extent of the low-N_2O waters from the OMZ's core was shifted to shallower depths within the center of mode water eddies A and B. More-

BGD
12, 9243–9273, 2015

over, shallower minima of N_2O were observed in the upper OMZ for stations located in the center of eddy A (150 m) compared to eddy B (250 m), whereas in both cases the second N_2O minima were slightly displaced towards deeper depths. N_2O concentrations at the boundaries of the OMZ in the center of eddy A were similar to those in its edge, whereas for eddy B the N_2O concentrations in the center were markedly lower than in its edge and outside of it. N_2O decrease at the core of the OMZ (defined as the depth range with $O_2 < 20\,\mu mol\,L^{-1}$) was, however, stronger in the center of both anticyclonic eddies A and B with respect to stations at their edges (Fig. 3), suggesting enhanced N_2O consumption. This is consistent with observations from Stramma et al. (2013) who reported active N-loss processes based on the co-occurrence of pronounced NO_2^- maxima as well as O_2 and NO_3^- minima at the core of the OMZ within the center of both eddies A and B. Stramma et al. (2013) suggested a decline in N-loss activity in eddy B compared to eddy A, arguing that nutrient subduction along with reduced productivity might have reduced the flux of organic matter that could fuel these processes when the eddies move towards the open ocean. According to this, a comparatively lower consumption of N_2O by denitrification within the OMZ in center of eddy B should diminish the differences between profiles inside and outside. However, this effect was not visible in the N_2O distribution and conversely, N_2O concentrations were generally lower in the center of eddy B than in the center of eddy A. While depth-integrated N_2O concentration in the OMZ within the open ocean eddy B was only 6 % lower than in coastal eddy A, observed differences were as high as 25 % when the entire water column (5–1000 m) was considered. This result can be explained by lower water column O_2 concentrations in eddy A than in eddy B (36.4 and 42.9 $mol\,m^{-2}$, respectively) since this might have favored enhanced N_2O production in eddy A at the oxic-suboxic boundaries (see Sect. 4.2), thus compensating for the N_2O depletion in the OMZ core. Hence, although a general decrease in organic matter turnover in open ocean eddy B was observed (Stramma et al., 2013), during our survey this was not evident for N_2O. This could either reflect dissimilarities of the water masses in both eddies at the time of formation (see Sect. 4.3), or slower denitrification rates in the edges of

BGD
12, 9243–9273, 2015

eddy B than in its center. A decreased pace of denitrification could explain the higher N_2O concentration in the OMZ from stations outside of eddy B than those in its center because it would imply slower N_2O consumption (transformation to N_2).

Vertical distribution of N_2O in eddy C was similar to that of the two anticyclonic eddies, with doming of isopycnals in its center causing a shift of the upper and lower N_2O maxima, although in this case towards shallower depths. We found elevated N_2O concentrations at the boundaries of the OMZ and only a slight decrease at 150–400 m depth, where O_2 concentrations fell below 5 µmol L^{-1} (Fig. 3). Nonetheless, N_2O minimum at the core of the OMZ was less pronounced than for eddies A and B, and the N_2O concentrations were higher in the eddy's center than in its edge. Analysis of SSHA data showed, however, that stations assumed to be located in the edge and outside of eddy C were actually influenced by another anticyclonic eddy, and therefore are not representative of the mean conditions at the ETSP. Our results are consistent with the observations of Stramma et al. (2013) who reported elevated O_2 concentrations as well as low NO_2^- accumulation at the center of eddy C, suggesting lower activity of N-loss processes than in eddies A and B. Although upon formation cyclonic eddies tend to increase subsurface production as mode water eddies do, this effect is not long-lasting and the net downwelling of nutrients ultimately leads to decreased primary productivity (McGillicuddy Jr. et al., 2007). Therefore it is likely that the decaying primary production of eddy C during its transit away from the shelf led to a diminished supply of organic matter which could fuel N-loss within the OMZ's core, explaining the relatively high N_2O concentrations observed in comparison to eddies A and B. Both our maximum and minimum of N_2O concentrations along the vertical O_2 gradient were well within the range of previous observations in the ETSP (Farías et al., 2007, 2009), although our values for the coastal eddy A were somewhat lower, probably reflecting the influence of coastal upwelling events during their sampling.

Despite the fact that high N_2O concentrations were produced on and above the upper oxycline, and that shoaling of isoclines in the upper 100 m of eddy A was at some extent visible in the N_2O vertical profiles, these features do not appear in near-surface waters

BGD
12, 9243–9273, 2015

like they do during coastal upwelling on the shelf. We found that during our survey the exceptionally high N_2O concentrations in the near-surface corresponded to stations located closer to the coast and thus out of the influence of eddy A. Furthermore, we observed a markedly different profile type for coastal stations, wherein a rapid decrease in O_2 concentrations (OMZ start at about 15 m depth) was followed by a narrow peak in N_2O between 10 and 40 m depth (Fig. 3). Hence, although mesoscale eddies seem to influence the vertical distribution of N_2O, they do not have a direct impact on its surface distribution and emissions to the atmosphere since they are "trapped" below the mixed layer.

4.2 N_2O cycling within coastal eddy A

SSHA data from December 2012 indicated that coastal mode water eddy A was still centered near the shelf break at about 16° 30'S, 76°30′ W. The O_2 distribution along a cross-shelf section between 16°9′ S, 76°50′ W and 15°23′ S, 75°20′ W revealed O_2 minima not only in the center of eddy A, but also in the vicinity of the shelf break due to coastal upwelling. (Fig. 4). An intermediate-depth low N_2O layer was consistent with the location of low O_2 ($< 5\,\mu mol\,L^{-1}$) waters and it reached its maximum extension (70–400 m depth) close to the western side of eddy A center. Although a strong maximum of N_2O (up to $80\,nmol\,L^{-1}$) could be observed at about 40 m depth within the station located in the center of the eddy, the subsequent and sharp decrease in O_2 concentrations led to a marked decrease in N_2O.

The observed NO_3^- and N^* minima, as well as the pronounced secondary nitrite maximum (Codispoti and Packard, 1980) were consistent with the N_2O distribution, suggesting the occurrence of strong N-loss processes, particularly in the center of eddy A. Abundances of the *hzo* gene (encoding for hydrazine oxidoreductase), which is the functional gene marker for anaerobic ammonium oxidation (anammox; Schmid et al., 2008), were generally higher through the water column within the center of eddy A, and the maxima were found at shallower depths (50 and 200 m depth) than outside (Fig. 5). Although anammox does not reflect N_2O consumption, it does provide an indication of

BGD
12, 9243–9273, 2015

active N-loss within the OMZ of the eddy at the time of sampling (Dalsgaard et al., 2012; De Brabandere et al., 2014) and therefore supports the observations from Altabet et al. (2012) and Stramma et al. (2013) in the ETSP.

Active nitrification, as indicated by the depth distribution of gene abundances of *amoA*, the functional key gene for archaeal ammonium oxidation (Löscher et al., 2012), was observed within eddy A, and was stronger in the upper 200 m for the center of the eddy, whereas below 200 m it was of similar magnitude for stations outside and in the center (Fig. 5). This would explain the comparatively high, shallow-depth maximum of N_2O within the center of eddy A (Fig. 4). Based on the structure of the vertical profiles of *nirS* gene abundances, we could also infer that N_2O maxima at the boundaries of the OMZ partially resulted from production during early stages of denitrification. Our observations support the results of Castro-González and Farías (2004), who used N_2O production experiments in the ETSP to show that denitrifiers produce increasing $N_2O : N_2$ ratios as the O_2 concentrations increase due to the well-known sensitivity of the N_2O reductase to O_2 (Dalsgaard et al., 2014). Furthermore, except for a deep minimum at 600 m, N_2O production (as inferred from *nirS* abundances) was stronger in the center of the eddy (Fig. 5). Nevertheless, within the OMZ's core it was evident that N_2O consumption was stronger in the center of the eddy, suggesting that even though the genes for N_2O production by denitrification were present, they were probably inhibited due to further low O_2 concentrations ($\sim 3\,\mu mol\,L^{-1}$). It is also likely, however, that under denitrifying conditions N_2O depletion occurs at a faster rate than production, masking the N_2O production signal. Elevated NO_2^- concentrations ($11\,\mu mol\,L^{-1}$) along with close to detection limit NO_3^- concentrations in the OMZ further suggests that complete -and more intense- denitrification took place in the OMZ core at the eddy center (Codispoti and Christensen, 1985; Codispoti et al., 1986). Thus, in general, in the center of the eddy a higher N_2O maxima at the upper boundary of the OMZ resulted from enhanced nitrification and partial denitrification, whereas stronger N_2O depletion at the OMZ's core resulted from enhanced, complete denitrification. Although at depths below 600 m both *amoA* and *nirS* gene abundances were higher outside of the eddy, N_2O concentra-

BGD
12, 9243–9273, 2015

tions remained similar to those in the center and O_2 was still lower in the eddy's center (Fig. 5). Nevertheless, vertical profiles of the same eddy one month before showed that N_2O concentrations below 600 m were higher in the center (cf. Fig. 3). Thus, it could be that increasing variability beneath the lower boundary of the OMZ was caused by decreasing intensity (velocity) of the eddy below 600 m (Fig. 2). Overall, the net effect of anticyclonic eddy A was an enhancement of N-loss processes within its center, thereby making the OMZ's core an even stronger sink for N_2O than it would be under "mean" conditions.

4.3 Effect of eddy "aging" on N_2O

Westward propagation of mesoscale eddies implies that properties of the waters which were "enclosed" within its center at the time of formation are transported offshore (Chelton et al., 2007). Gruber et al. (2011) suggested that this transport leads to a net reduction of primary productivity in coastal upwelling regions due to nutrient subduction and advection. Since the export of organic matter is the most important factor fueling the N-cycling in the OMZ (Capone and Hutchins, 2013), changes in the distribution of the main production/consumption pathways of N_2O are likely to occur under the influence of mesoscale eddies during their transit to open waters. On the following we compare the vertical distributions of N_2O and relevant biogeochemical parameters within the center of the "young" coastal eddy A during the M90 cruise, and the "old" open ocean eddy B. Likewise, we include data of a second survey of eddy A during the M91 cruise (hereafter eddy A-M91). The cyclonic eddy C is not considered for this analysis given its relatively minor importance for N-loss processes.

Integrated concentration of N_2O within the center of the eddies was 24 and 53 % higher in eddy A than in eddy B and eddy A-M91, respectively (Table 1). In this case the difference between eddies A and B can be partially attributed to the location of formation and also to the fact the N-cycling processes tend to decrease after subsurface nutrients are subducted and primary production progressively decreases towards the open ocean. This is supported by higher O_2 and NO_3^- concentrations in eddy B than

BGD
12, 9243–9273, 2015

in eddy A, as well as the comparatively lower NO_2^- concentrations in eddy B, which suggests an overall decrease in organic matter respiration in the open ocean eddy. On the other hand, the marked decrease of N_2O in the coastal mode water eddy A only one month after the first sampling points towards an enhancement of N-loss processes within the OMZ of this eddy. In agreement with this observation, eddy A-M91 featured the lowest concentrations of O_2 and NO_3^-, as well as the highest NO_2^- values among the three eddies considered (Table 1). A substantial increase in abundances of both *amoA* and *nirS* genes was observed in the center of eddy A-M91 with respect to eddies A and B, explaining the comparatively higher N_2O concentrations found at the boundaries of the OMZ. It seems however, that enhanced N_2O production by nitrification and partial denitrification in eddy A-M91 is outpaced by high N_2O consumption in the core of the OMZ with further decreasing O_2 concentrations, which in turn resulted in values even lower than those of the open ocean eddy B. Furthermore, sharp differences in *hzo* gene abundances among the three eddies, with A-M91 featuring significantly higher values (Table 1), put in evidence that N-loss activities in the ETSP were comparatively stronger in coastal eddies at the time of sampling. Likewise this also suggests that strengthening of eddy A (increased velocity) while it stayed stationary on the shelf between the two surveys (M90 and M91) might have led to an N-cycling intensification through the water column.

In order to provide a quantitative estimate of the amount of denitrification that took place in eddy A, as well as to assess how it changed between the two surveys, we computed the nitrate deficit (ΔN) by means of the "NO" approach (Naqvi and Gupta, 1985). "NO" is used as a quasi-conservative water mass tracer (Broecker, 1974) and it is defined here as: $[O_2] + 9.1[NO_3^-]$ (Bange et al., 2000). A plot of "NO" vs. potential temperature (θ) from stations located at the center of eddy A during M90 and M91 is shown in Fig. 6. For both cruises we obtained a good correlation between "NO" and θ after excluding data points from the surface to the upper limit of the OMZ ($O_2 \sim 20\,\mu mol\,L^{-1}$), as well as those from the OMZ's core ($O_2 < 5\,\mu mol\,L^{-1}$). Hence, the obtained regression lines ("NO"$_{M90}$, "NO"$_{M91}$, Fig. 6) represent conditions which are expected when the

BGD
12, 9243–9273, 2015

OMZ is not affected by denitrification (Naqvi and Gupta, 1985). We calculated ΔN by using "NO"$_{M90}$ and "NO"$_{M91}$ according to the following expression (Bange et al., 2000): (["NO"$_x$] – [O_2]) / 9.1 – [NO_3^-] – [NO_2^-], where x is the corresponding regression line for each cruise.

After integrating ΔN over the depth range of the OMZ, we obtained values of 8.9 and 0.02 mol m^{-2} for eddy A during M90 and M91, respectively. ΔN from M90 was considerably higher than most estimates available for a similar OMZ in the Arabian Sea (Naqvi and Gupta, 1985; Howell et al., 1997; Bange et al., 2000), and it was only comparable with values up to 7.3 mol m^{-2} found by Naqvi and Gupta (1985) at about 20° N towards the coast of Oman. ΔN from M91 was however, markedly lower than both ΔN from M90 and ΔN from previous work in the OMZ of the Arabian Sea (minimum ΔN = 1.0 mol m^{-2}; Bange et al., 2000). This suggests not only strong denitrification activities within mesoscale eddies formed off the Peruvian coast, but also high short-term variability as they move offshore. Thus, the observed contrast in O_2, nutrients and N_2O integrated concentrations between eddy A and eddy A-M91 (Table 1), can be explained by the temporal differences in the strength of the denitrification processes in the OMZ's core within this coastal eddy. Hence, the evidence of N-loss observed during M91 does not reflect enhanced denitrification within the eddy at the time of sampling (December), but rather the remaining signal of strong denitrification during early stages of the eddy which were partially captured when we sampled it in November. Nevertheless, a pronounced Chl *a* and turbidity maximum in the center of eddy A-M91 suggest a potentially increased supply of organic matter which, upon sinking, could stimulate N-loss through anammox and denitrification (Kalvelage et al., 2013; De Brabandere et al., 2014). Therefore it is likely that N-loss still took place in the coastal eddy A during M91, although at rates comparatively lower than those during M90 and the time period elapsed between the two cruises.

In order to roughly estimate the amount of N-loss through denitrification which was driven by coastal eddy A between November and December 2012 (27 days), we used our ΔN values and a calculated area of 8.5 × 10^9 m^2. This resulted in a daily loss flux of

BGD
12, 9243–9273, 2015

0.04 Tg-N day^{-1}, which if scaled to an annual basis would be comparable with values reported for the Arabian Sea by Mantoura et al. (1993) but lower than most estimates for the same area (Naqvi, 1987; Howell et al., 1997; Bange et al., 2000) and for the eastern tropical South and North Pacific (20–33 and 20–29 Tg-N yr^{-1}, respectively; Codispoti and Richards, 1976; Codispoti and Packard, 1980; DeVries et al., 2012). However, a direct comparison with those studies is not entirely realistic since the mean lifespan of mesoscale eddies off Peru is typically not longer than a few months (Chaigneau et al., 2008). Therefore the intense N-loss observed within the eddies might represent a transient state which at times contributes significantly to the total N-loss in the ETSP. Since denitrification can also be a source of N_2O (Codispoti and Christensen, 1985; Bakker et al., 2014) we estimated the N_2O production from denitrifying waters within the OMZ's core ($O_2 < 5$ µmol L^{-1}) of eddy A. For this, we calculated the depth-integrated N_2O anomaly ($\Delta N_2O = N_2O_{measured} - N_2O_{equilibrium}$) over the OMZ for both profiles at the center of eddy A (M90 and M91). Using the eddy area and time span between cruises as shown above, we obtained a N_2O daily yield of 1.3×10^{-5} Tg-N_2O day^{-1} (or 8.0×10^{-6} Tg-N day^{-1}). Scaling this value to an annual basis resulted in a N_2O yield of 4.5×10^{-3} Tg-N_2O yr^{-1} (or 2.9×10^{-3} Tg-N yr^{-1}), which is markedly lower than previous values for the Arabian Sea (Mantoura et al 1993; Bange et al., 2001). Accordingly, our estimated N_2O production from denitrification is considerably low in comparison with our estimated denitrification rates from eddy A in November-December 2012 (0.02 %), suggesting faster N_2O consumption than production within the OMZ of eddy A for the period of sampling. N_2O production in the OMZ of the Arabian Sea has been reported to amount for at least 2 % of the mean denitrification rates (Bange et al, 2001). However this value is not entirely comparable with ours since in that study a whole basin (1.95×10^{12} m^2) is considered and our time span is in the order of months rather than years. It should be pointed out that our denitrification rates and N_2O yields from the OMZ assume a given size and permanence period of the eddy in coastal waters, and moreover, do not take in consideration the progressive decrease in N-loss activities within the eddy center as it moves away from the coast. Therefore, our values are only

BGD
12, 9243–9273, 2015

contentious and are meant to highlight the need of combined biogeochemical-physical studies which account for the annual variability in occurrence, abundance and spatial extent of mesoscale anticyclonic eddies off Peru, given their importance for N-loss processes.

The coastal eddy A was formed on the shelf about two months before the time of sampling, whereas the open ocean eddy B was formed at least five months before our survey. This hampers a direct comparison of both mode water eddies, in particular because with our methods it was not possible to determine the exact location where eddy B was formed. Nonetheless, the main physical and biogeochemical features of eddies A and B suggest that, in general, the "aging" of mesoscale eddies tends to decrease N_2O concentrations through the water column in response to reduced supply of material to fuel microbial respiration in the boundaries of the OMZ. Hence, the comparatively lower N_2O depletion due to N-loss through denitrification in the OMZ core of open ocean eddies does not match the reduced N_2O production in its boundaries. Water mass properties at the time of formation, however, might account for the observed differences between eddies recently formed on the shelf and those in the open ocean. On the other hand, the pace at which the different microbial pathways leading to N_2O production/consumption develop can be also influenced by the spatial and temporal variability of the physical setup on the mesoscale feature while moving offshore.

5 Summary and conclusions

In this study we used a combined approach including physical, biogeochemical and molecular methods in order to investigate the distribution of N_2O within mesoscale eddies in the ETSP. Overall, a "two peak" structure was observed in vertical profiles of N_2O, indicating the alternation between production and consumption processes as a response to the O_2 gradients through the water column. Our results suggest that N_2O concentrations in the water column were consistent with the main physical features of the mesoscale eddies. Hence, lifting/deepening of the seasonal/main pycnoclines in

BGD
12, 9243–9273, 2015

mode water eddies (A and B) was visible for N_2O, with shoaling of the upper maxima and slight displacement of the lower maxima towards deeper depths. Likewise, doming of isopycnals in the open ocean cyclonic eddy (C) caused a shift of the upper and lower N_2O maxima towards shallower depths. O_2 and nutrient (NO_3^- and NO_2^-) distributions as well as abundances of key gene markers for N_2O production processes showed that the upper and lower oxyclines in the boundaries of the OMZ are net sources of N_2O, producing the two observed maxima which envelop the N_2O-depleted waters in the core of the OMZ. Nitrification combined with incomplete denitrification was responsible for the N_2O maxima, whereas active denitrification led to a net consumption of N_2O. Trapping of highly productive coastal waters in anticyclonic eddies (e.g. eddy A) led to a net enhancement of N-loss processes in its center both through denitrification and anammox, thereby making the OMZ's core an even stronger sink for N_2O than it would be under "mean" conditions, and moreover creating hotspots for loss of bioavailable fixed N. However, the strength of the N-cycling processes decreases during the transit of the eddies out of the shelf, mostly in response to a lower supply of organic matter from surface waters and sinking of nutrients as the eddy collapses. Hence our observations suggest that open ocean mode waters eddies tend to produce less N_2O than coastal ones because the weaker maxima that enclose the OMZ core have an overall bigger impact than the reduced N_2O consumption within the OMZ core. Nevertheless, water properties at the time of formation, as well as the pace at which eddies propagate might alter the N_2O concentrations through the water column. Although depth distribution of N_2O in the center of cyclonic eddy C was similar to eddies A and B, in general the concentrations (both maxima and minima) were higher and its relative importance for N-loss was negligible. Despite of the observed shoaling of upper isopycnals in both mode water and cyclonic eddies, we did not find any appreciable changes in the surface distribution of N_2O since these features are trapped below the mixed layer.

In conclusion, our survey provides the first insights of N_2O distribution within mesoscale eddies in the ETSP, and points out the importance of multidisciplinary ap-

BGD
12, 9243–9273, 2015

proaches in investigating the rather multifaceted N-cycling in OMZs. However, high complexity of the N_2O production and consumption pathways together with unaccounted temporal and spatial variability, hamper the chances of an objective quantification of the net effect of mesoscale eddies in N_2O for the whole ETSP. Projected future deoxygenation and expansion of OMZs has been suggested to significantly increase marine N_2O production. However, an increased strength of the N_2O sink within the core of low-O_2 waters in mesoscale eddies might also play an important role which has not been yet quantified. Hence, it is critical to understand how these prominent features of the circulation might affect N_2O distribution and concentrations in order to be able to assess the variability of its sources and sinks strength.

Author contributions. L. Stramma, D. L. Arévalo-Martínez, and H. W. Bange conceived the study; D. L. Arévalo-Martínez set up the instrumentation for discrete N_2O measurements on board of the R/V *Meteor* and carried out the field work together with A. Kock and H. W. Bange. D. L. Arévalo-Martínez and A. Kock processed and calibrated depth profile N_2O data. C. R. Löscher collected and processed the molecular data. L. Stramma processed and analyzed hydrographic data. D. L. Arévalo-Martínez wrote the manuscript with contributions from H. W. Bange, A. Kock, C. R. Löscher, R. A. Schmitz, and L. Stramma.

Acknowledgements. This study was funded by the DFG-supported project SFB754 (http://www.sfb754.de), the BMBF joint project SOPRAN II and III (FKZ 03F0611A and FKZ 03F662A), and the EU FP7 project InGOS (Grant Agreement # 284274). We thank the Peruvian authorities for authorizing us to conduct the study in their territorial waters. We also would like to thank our Peruvian colleagues from IMARPE (M. Graco, A. Bernal, G. Flores and V. León) for their logistical support. We thank the captains and crew of the R/V *Meteor* for their assistance during the cruises M90 and M91. Likewise, we thank T. Baustian, A. Bernal, J. Craig, G. Eirund, G. Flores, V. León, M. Lohmann, N. Martogli, K. Nachtigall and G. Krahmann for their contributions to the processing of the different data sets used in this study. Analyses and visualizations of Chlorophyll used in this study (Fig. 1) were produced with the Giovanni online data system, developed and maintained by the NASA GES DISC. The altimeter data were produced by Ssalto/Duacs and distributed by Aviso with support from Cnes.

BGD
12, 9243–9273, 2015

References

Altabet, M. A., Ryabenko, E., Stramma, L., Wallace, D. W. R., Frank, M., Grasse, P., and Lavik, G.: An eddy-stimulated hotspot for fixed nitrogen-loss from the Peru oxygen minimum zone, Biogeosciences, 9, 4897–4908, 2012, http://www.biogeosciences.net/9/4897/2012/.

Arévalo-Martínez, D. L., Beyer, M., Krumbholz, M., Piller, I., Kock, A., Steinhoff, T., Körtzinger, A., and Bange, H. W.: A new method for continuous measurements of oceanic and atmospheric N_2O, CO and CO_2: performance of off-axis integrated cavity output spectroscopy (OA-ICOS) coupled to non-dispersive infrared detection (NDIR), Ocean Sci., 9, 1071–1087, 2013, http://www.ocean-sci.net/9/1071/2013/.

Bakker, D. C. E., Bange, H. W., Gruber, N., Johannenssen, T., Upstill-Goddard, R. C., Borges, A. V., Delille, B., Löscher, C. R., Naqvi, S. W. A., Omar, A. O., and Santana-Casiano, J. M.: Air-sea interactions of natural long-lived greenhouse gases (CO_2, N_2O, CH_4) in a changing climate, in: Ocean-atmosphere interactions of gases and particles, edited by: Liss, P. S. and Johnson, M. T., 113–169, Springer, Heidelberg, 2014.

Bange, H. W., Rixen, T., Johansen, A. M., Siefert, R. L., Ramesh, R., Ittekkot, V., Hoffmann, M. R., and Andreae, M. O.: A revised nitrogen budget for the Arabian Sea, Global Biogeochem. Cy., 14, 1283–1297, 2000.

Bange, H. W., Rapsomanikis, S., and Andreae, M. O.: Nitrous oxide cycling in the Arabian Sea, J. Geophys. Res., 106, 1053–1065, 2001.

Bange, H. W., Freing, A., Kock, A., and Löscher, C. R.: Marine pathways to nitrous oxide, in: Nitrous oxide and climate change, edited by: Smith, K., 36–62, Earthscan, London, 2010.

Broecker, W. S.: "NO", a conservative water-mass tracer, Earth Planet. Sci. Lett., 23, 100–107, 1974.

De Brabandere, L., Canfield, D. E., Dalsgaard, T., Friederich, G. E., Revsbech, N. P., Ulloa, O., and Thamdrup, B.: Vertical partitioning of nitrogen-loss processes across the oxic-anoxic interface of an oceanic oxygen minimum zone, Environ. Microbiol., 16, 3041–3054, 2014.

DeVries, T., Deutsch, C., Primeau, F., Chang, B., and Devol, A.: Global rates of water-column denitrification derived from nitrogen gas measurements, Nat. Geosci., 5, 547–550, 2012.

Capone, D. G. and Hutchins, D. A.: Microbial biogeochemistry of coastal upwelling regimes in a changing ocean, Nat. Geosci., 6, 711–717, 2013.

BGD
12, 9243–9273, 2015

Castro-González, M. and Farías, L.: N_2O cycling at the core of the oxygen minimum zone off northern Chile, Mar. Ecol.-Prog. Ser., 280, 1–11, 2004.
Chaigneau, A., Gizolme, A., and Grados, C.: Mesoscale eddies off Peru in altimeter records: Identification algorithms and eddy spatio-temporal patterns, Prog. Oceanogr., 79, 106–119, 2008.
Chelton, D. B., Schlax, M. G., Samelson, R. M., and de Szoeke, R. A.: Global observations of large oceanic eddies, Geophys. Res. Lett., 34, L15606, doi:10.1029/2007GL030812, 2007.
Chelton, D. B., Gaube, P., Schlax, M. G., Early, J. J., and Samelson, R. M.: The influence of nonlinear mesoscale eddies on near-surface oceanic chlorophyll, Science, 334, 328–332, 2011.
Codispoti, L. A.: Interesting times for marine N_2O, Science, 327, 1339–1340, 2010.
Codispoti, L. A. and Christensen, J. P.: Nitrification, denitrification and nitrous oxide cycling in the eastern tropical South Pacific Ocean, Mar. Chem., 16, 277–300, 1985.
Codispoti, L. A. and Packard, T. T.: Denitrification rates in the eastern tropical South Pacific, J. Mar. Res., 38, 453–477, 1980.
Codispoti, L. A. and Richards, F. A.: An analysis of the horizontal regime of denitrification in the eastern tropical North Pacific, Limnol. Oceanogr., 21, 379–388, 1976.
Codispoti, L. A., Friederich, G. E., Packard, T. T., Glover, H. E., Kelly, P. J., Spinrad, R. W., Barber, R. T., Elkins, J., W., Ward, B. B., Lipschultz. F., and Lostaunau, N.: High nitrite levels off northern Peru: a signal of instability in the marine denitrification rate, Science, 233, 1200–1202, 1986.
Correa-Ramirez, M. A., Hormazábal, S., and Yuras, G.: Mesoscale eddies and high chlorophyll concentrations off central Chile (29°–39° S), Geophys. Res. Lett., 34, L12604, doi:10.1029/2007GL029541, 2007.
Dalsgaard, T., Thamdrup, B., Farías, L., and Revsbech, N. P.: Anammox and denitrification in the oxygen minimum zone of the eastern South Pacific, Limnol. Oceanogr., 57, 1331–1346, 2012.
Dalsgaard, T. Stewart, F. J., Thamdrup, B., De Brabandere, L., Revsbech, N. P., Ulloa, O., Canfield, D. E., and DeLong, E. F.: Oxygen at nanomolar levels reversibly suppresses process rates and gene expression in anammox and denitrification in the oxygen minimum zone off northern Chile, mBio, 5, e01966-14, doi:10.1128/mBio.01966-14, 2014.
Deutsch, C., Brix, H., Ito, T., Frenzel, H., and Thompson, L.: Climate-forced variability of ocean hypoxia, Science, 333, 336–339, 2011.

BGD
12, 9243–9273, 2015

Falkowski, P. G.: Evolution of the nitrogen cycle and its influence on the biological sequestration of CO_2 in the ocean, Nature, 387, 272–275, 1997.
Farías, L., Paulmier, A., and Gallegos, M.: Nitrous oxide and N-nutrient cycling in the oxygen minimum zone off northern Chile, Deep-Sea Res. Pt. I, 54, 164–180, 2007.
Farías, L., Castro-González, M., Cornejo, M., Charpentier, J., Faúndez, J., Boontanon, N., and Yoshida, N.: Denitrification and nitrous oxide cycling within the upper oxycline of the eastern tropical South Pacific oxygen minimum zone, Limnol. Oceanogr., 54, 132–144, 2009.
Goreau, T. J., Kaplan, W. A., Wofsky, S. C., McElroy, M. B., Valois, F. W., and Watson, S. W.: Production of NO_2^- and N_2O by nitrifying bacteria at reduced concentrations of oxygen, Appl. Environ. Microb., 40, 526–532, 1980.
Gruber, N., Lachkar, Z., Frenzel, H., Marchesiello, P., Münnich, M., McWilliams, J. C., Nagai, T., and Plattner, G.-K.: Eddy-induced reduction of biological production in eastern boundary upwelling systems, Nat. Geosci., 4, 787–792, 2011.
Hansen, H. P.: Determination of oxygen, in: Methods of Seawater Analysis, edited by: Grasshoff, K. G., Kremling, K., and Ehrhardt, M., Wiley-VCH, Weinheim, 75–90, 1999.
Howell, E. A., Doney, S. C., Fine, R. A., and Olson, D. B.: Geochemical estimates of denitrification in the Arabian Sea and the Bay of Bengal during WOCE, Geophys. Res. Lett., 24, 2549–2552, 1997.
Kalvelage, T., Lavik, G., Lam, P., Contreras, S., Arteaga, L., Löscher, C. R., Oschlies, A., Paulmier, A., Stramma, L., and Kuypers, M. M. M.: Nitrogen cycling driven by organic matter export in the South Pacific oxygen minimum zone, Nat. Geosci., 6, 228–234, 2013.
Karstensen, J., Stramma, L., and Visbeck, M.: Oxygen minimum zones in the eastern tropical Atlantic and Pacific oceans, Prog. Oceanogr., 77, 331–350, 2008.
Löscher, C. R., Kock, A., Könneke, M., LaRoche, J., Bange, H. W., and Schmitz, R. A.: Production of oceanic nitrous oxide by ammonia-oxidizing archaea, Biogeosciences, 9, 2419–2429, doi:10.5194/bg-9-2419-2012, 2012.
Löscher, C. R., Großkopf, T., Desai, F. D., Gill, D., Schunck, H., Croot, P. L., Schlosser, C., Neulinger, S. C., Pinnow, N., Lavik, G., Kuypers, M. M. M., LaRoche, J., and Schmitz, R. A.: Facets of diazotrophy in the oxygen minimum zone waters off Peru, The ISME Journal, 8, 2180–2192, 2014.
Löscher, C. R., Bange, H. W., Schmitz, R. A., Callbeck, C. M., Engel, A., Hauss, H., Kanzow, T., Kiko, R., Lavik, G., Loginova, A., Melzner, F., Neulinger, S. C., Pahlow, M., Riebesell, U., Schunck, H., Thomsen, S., and Wagner, H.: Water column biogeochemistry of oxygen mini-

BGD
12, 9243–9273, 2015

mum zones in the eastern tropical North Atlantic and eastern tropical South Pacific Oceans, Biogeosciences Discuss., 12, 4495–4556, doi:10.5194/bgd-12-4495-2015, 2015.
McGillicuddy Jr., D. J., Anderson, L. A., Bates, N. R., Bibby, T., Buesseler, K. O., Carlson, C. A., Davis, C. S., Ewart, C., Falkowski, P. G., Goldthwait, S. A., Hansell, D. A., Jenkins, W. J., Johnson, R., Kosnyrev, V. K., Ledwell, J. R., Li, Q. P., Siegel, D. A., and Steinberg, D. K.: Eddy/wind interactions stimulate extraordinary mid-ocean plankton blooms, Science, 316, 1021–1026, 2007.
Mantoura, R. F. C., Law, C. S., Owens, N. J. P., Burkill, P. H., Woodward, E. M. S., Howland, R. J. M., and Llewellyn, C. A.: Nitrogen biogeochemical cycling in the northwestern Indian Ocean, Deep-Sea Res. Pt. II, 40, 651–671, 1993.
Myhre, G. D., Schindell, D., Bréon, F.-M., Collins, W., Fuglestvedt, J., Huang, J., Koch, D., Lamarque, J.-F., Lee, D., Mendoza, B., Nakajima, T., Robock, A., Stephens, G., Takemura, T., and Zhang, H.: Anthropogenic and natural radiative forcing, in: Climate Change 2013: The Physical Science Basis, Contribution of Working Group I to the Fifth Assessment Report of the Intergovernmental Panel on Climate Change, edited by: Stocker, T. F., Qin, D., Plattner, G.-K., Tignor, M., Allen, S. K., Boschung, J., Nauels, A., Xia, Y., Bex, V., and Midgley, P. M., Cambridge University Press, Cambridge, United Kingdom and New York, USA, 129–234, 2013.
Naqvi, S. W. A.: Some aspects of the oxygen-deficient conditions and denitrification in the Arabian Sea, J. Mar. Res., 45, 1049–1072, 1987.
Naqvi, S. W. A. and Gupta, R. S.: "NO", a useful tool for the estimation of nitrate deficits in the Arabian Sea, Deep-Sea. Res., 32, 665–674, 1985.
Naqvi, S. W. A., Bange, H. W., Farías, L., Monteiro, P. M. S., Scranton, M. I., and Zhang, J.: Marine hypoxia/anoxia as a source of CH_4 and N_2O, Biogeosciences, 7, 2159–2190, doi:10.5194/bg-7-2159-2010, 2010.
Paulmier, A., Ruiz-Pino, D., and Garcon, V.: The oxygen minimum zone (OMZ) off Chile as an intense source of CO_2 and N_2O, Cont. Shelf. Res., 28, 2746–2756, 2008.
Ravishankara, A. R., Daniel, J. S., and Portmann, R. W.: Nitrous oxide (N_2O): The dominant ozone-depleting substance emitted in the 21st Century, Science, 326, 123–125, 2009.
Schmid, M. C., Hooper, A. B., Klotz, M. G., Woebken, D., Lam, P., Kuypers, M. M. M., Pommerening-Roeser, A., Op den Camp, H. J. M., and Jetten, M. S. M.: Environmental detection of octahaem cytochrome c hydroxylamine/hydrazine oxidoreductase genes of aerobic and anaerobic ammonium-oxidizing bacteria, Environ. Microbiol., 10, 3140–3149, 2008.

BGD
12, 9243–9273, 2015

Stramma, L., Schmidtko, S., Levin, L. A., and Johnson, G. C.: Ocean oxygen minima expansions and their biological impacts, Deep-Sea Res. Pt. I, 57, 587–595, 2010.

Stramma, L., Bange, H. W., Czeschel, R., Lorenzo, A., and Frank, M.: On the role of mesoscale eddies for the biological productivity and biogeochemistry in the eastern tropical Pacific Ocean off Peru, Biogeosciences, 10, 7293–7306, doi:10.5194/bg-10-7293-2013, 2013.

Stramma, L., Weller, R. A., Czeschel, R., and Bigorre, S.: Eddies and an extreme water mass anomaly observed in the eastern south Pacific at the Stratus mooring, J. Geophys. Res.-Oceans, 119, 1068–1083, 2014.

Suntharalingam, P., Sarmiento, J. L., and Toggweiler, J. R.: Global significance of nitrous-oxide production and transport from oceanic low-oxygen zones: a modeling study, Global Biogeochem. Cy., 14, 1353–1370, 2000.

Walter, S., Breitenbach, U., Bange, H. W., Nausch, G., and Wallace, D. W. R.: Distribution of N_2O in the Baltic Sea during transition from anoxic to oxic conditions, Biogeosciences, 3, 557–570, doi:10.5194/bg-3-557-2006, 2006.

Welschmeyer, N.: Fluorometric analysis of Chlorophyll *a* in the presence of Chlorophyll *b* and phaeopigments, Limnol. Oceanogr., 39, 1985–1992, 1994.

BGD
12, 9243–9273, 2015

Table 1. Comparison of physical and biogeochemical properties of mode water eddies in the ETSP during the M90 (November 2012) and M91 (December 2012) cruises. N_2O, O_2, NO_3^-, NO_2^- and selected functional gene markers are expressed as integrated concentrations/abundances over the water column (0–600 m).

	A (M90)	A(M91)	B(M90)
Vertical extent (m)[a]	0–600	0–600	0–600
Radius (km)[a]	52.0	–	48.8
Volume (10^{12} m^3)[a]	5.2	–	4.7
N_2O (mol m^{-2})	0.034	0.016	0.026
O_2 (mol m^{-2})	36.4	10.8	42.9
NO_3^- (mol m^{-2})	14.8	12.4	15.8
NO_2^- (mol m^{-2})	1.6	2.6	0.52
amoA (10^8 copies m^{-2})	19.54	598.5	379.3
nirS (10^8 copies m^{-2})	0.37	57.9	0.23
hzo (10^8 copies m^{-2})	4.27	101773	2.9

[a] Values taken from Stramma et al. (2013).

BGD
12, 9243–9273, 2015

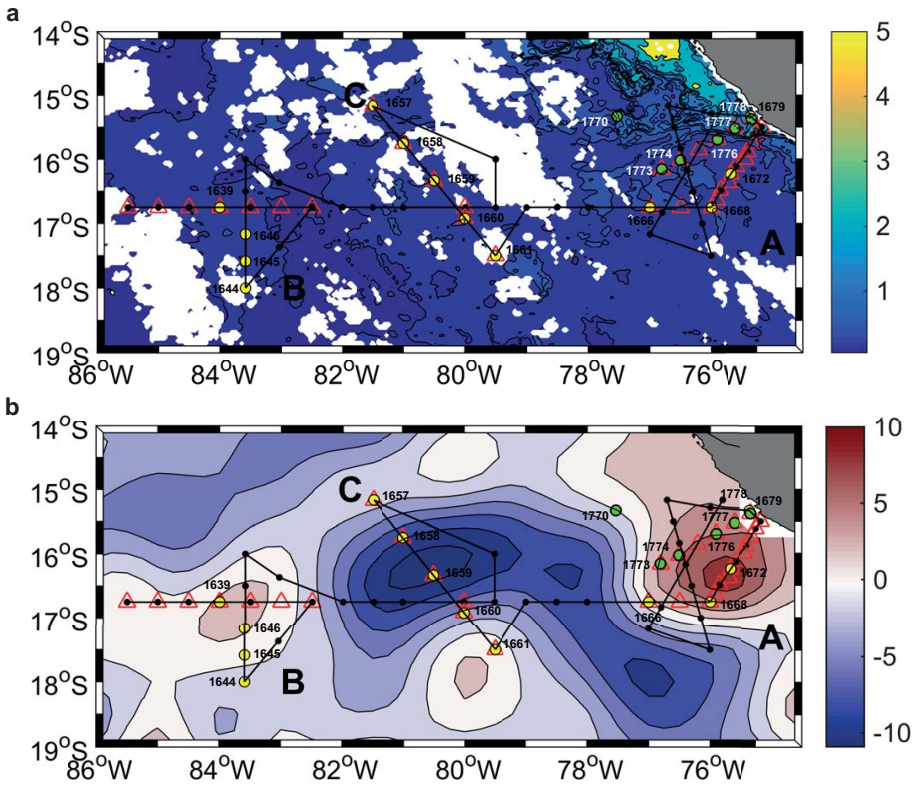

Figure 1. Map of sampling locations in the ETSP. **(a)** MODIS-Aqua 4 km monthly mean Chl *a* concentration (mg m^{-3}) for November-December 2012. **(b)** Aviso sea level height anomaly (cm) for the 21 November 2012 (anticyclonic eddies are depicted in red and cyclonic in blue). The cruise track and CTD stations with bottle sampling from the M90 cruise are shown in black. Open triangles indicate the hydrographic stations shown in Fig. 2. Sampling stations within the mode water eddies A and B, as well as the open ocean cyclonic eddy C are highlighted in yellow, whereas the cross-shelf section carried out during the M91 cruise is displayed in green.

BGD
12, 9243–9273, 2015

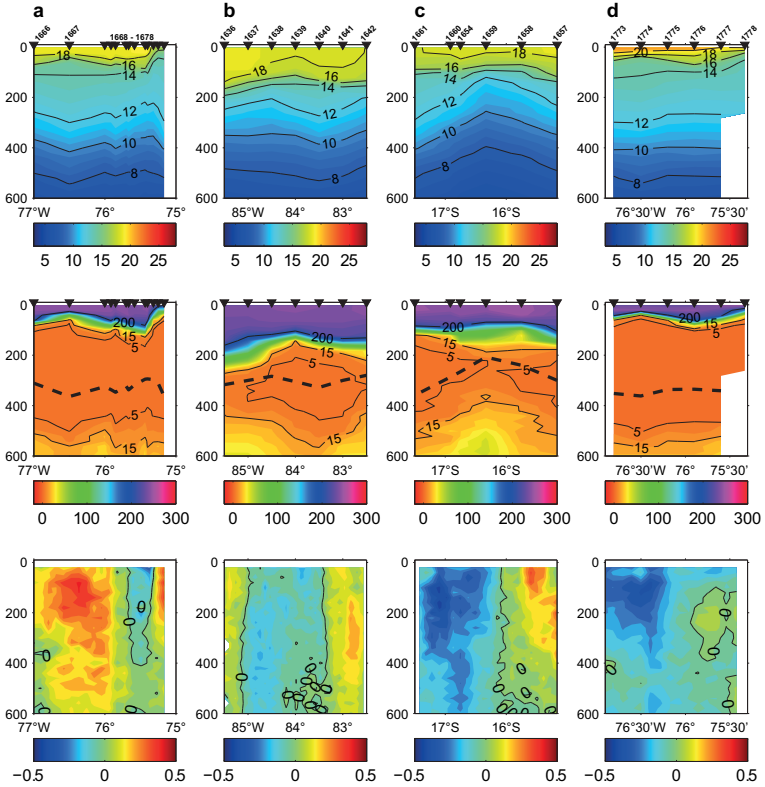

Figure 2. Hydrographic conditions at the time of sampling in the ETSP. Temperature in °C (upper panels), O_2 in µmol kg^{-1} (middle panels) and zonal **(a, c, d)**/meridional **(b)** velocity in m s^{-1} (lower panels) for eddies A, B and C during the M90 cruise (November 2012; **a–c**), as well as for eddy A during the M91 cruise (December 2012; **d**) are shown. Locations of CTD profiles are marked by black triangles (cf. Fig. 1) and the isopycnal $\sigma_\theta = 26.6\,\mathrm{kg\,m^{-3}}$ near the core of the OMZ is included in the O_2 sections as a black dashed line.

BGD
12, 9243–9273, 2015

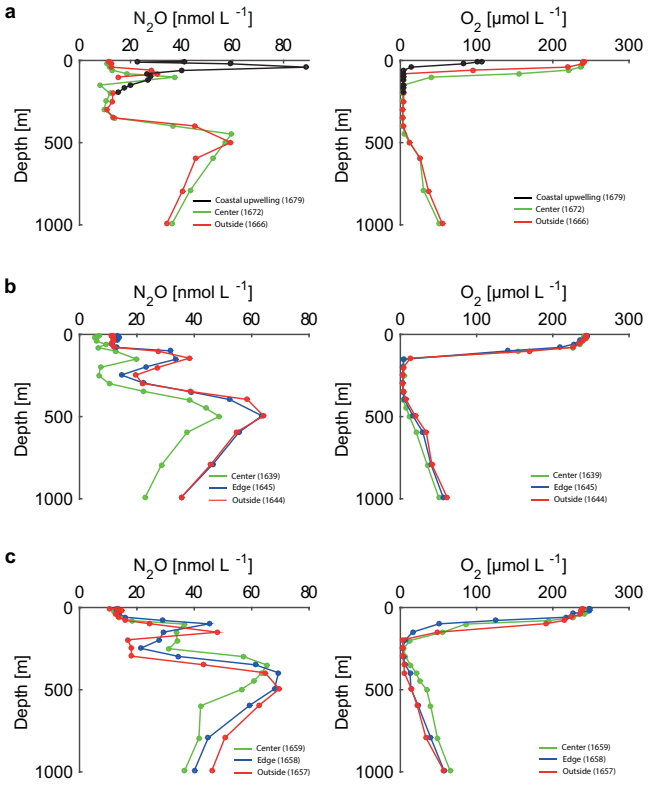

Figure 3. Selected depth profiles of N_2O (left) and O_2 (right) across the mode water eddies A **(a)**, B **(b)**, and the cyclonic eddy C **(c)** during the M90 cruise in November 2012. The sampling location is indicated by the different line/circle colors: green = center, blue = edge, red = outside. Black lines/symbols in **(a)** show the northwesternmost station of eddy A, in which the influence of coastal upwelling was observed. Numbers in parenthesis indicate the station numbers (cf. Fig. 1).

BGD
12, 9243–9273, 2015

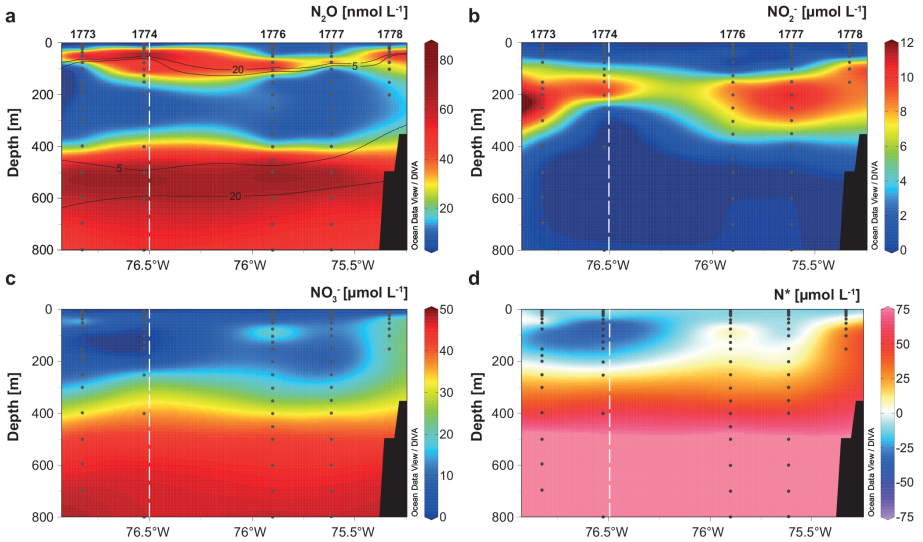

Figure 4. Cross-shelf distribution of N_2O **(a)**, NO_2^- **(b)**, NO_3^- **(c)** and N^* **(d)** along eddy A in December 2012 (16.2° S, 76.9° W to 15.3° S 75.2° W, see Fig. 1). Contours in **(a)** represent O_2 concentrations (in µmol L^{-1}). The white dashed lines indicate the approximate location of the eddy center according to SSHA data. Numbers above panels **(a)** and **(b)** are the station numbers (cf. Fig. 1).

BGD
12, 9243–9273, 2015

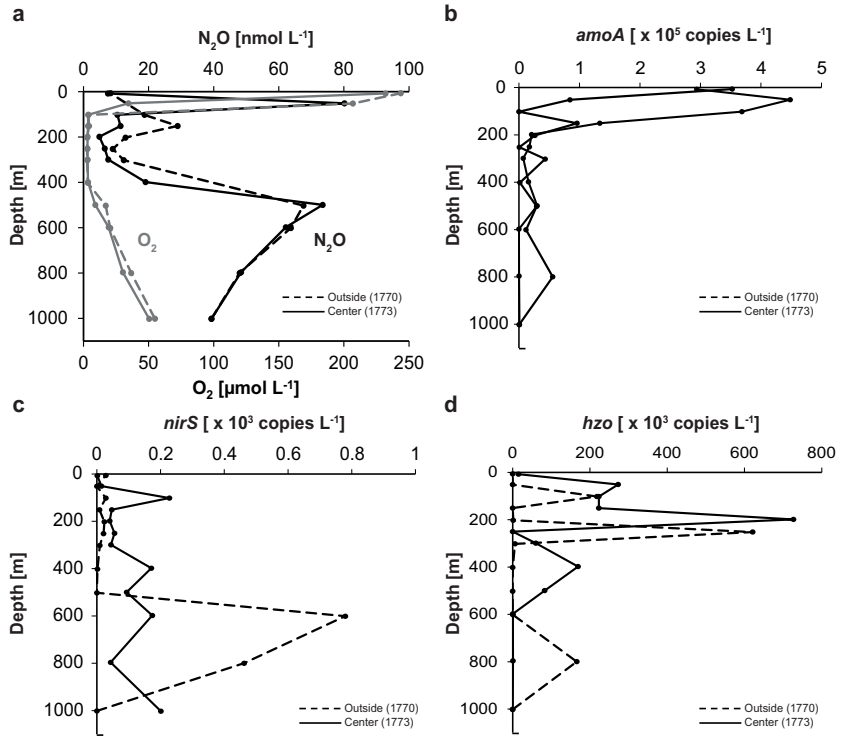

Figure 5. Vertical distribution of N_2O and O_2 concentrations **(a)**, as well as gene abundance of *amoA* **(b)**, *nirS* **(c)** and *hzo* **(d)** within the center (solid lines) and outside (dashed lines) of eddy A in December 2012 (M91 cruise). The numbers in parenthesis indicate the station numbers (cf. Fig. 1).

BGD
12, 9243–9273, 2015

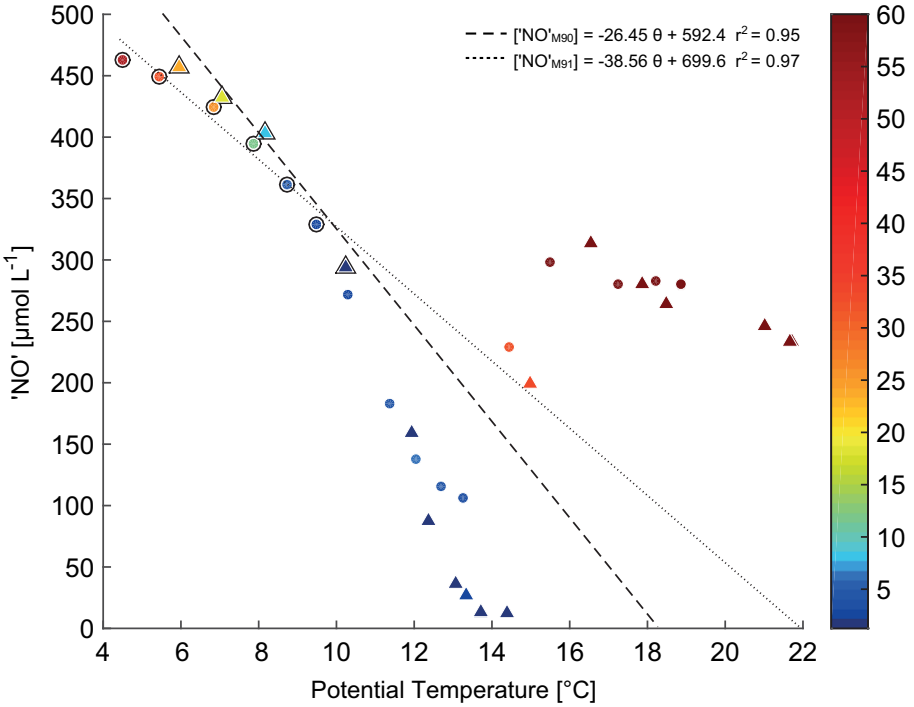

Figure 6. "NO" vs. potential temperature (θ) for stations located at the center of eddy A during M90 (November 2012; circles) and M91 (December 2012; triangles). The color bar represents the O_2 concentrations (scale has been truncated at 60 µmol L^{-1}). "NO" values from non-denitrifying waters ($O_2 > 5$ µmol L^{-1}) are highlighted in black and were used for the linear least-squares regressions.

BGD
12, 9243–9273, 2015